JACS JOURNAL OF THE AMERICAN CHEMICAL SOCIETY

Article

Cite This: J. Am. Chem. Soc. 2020, 142, 1321−1331

pubs.acs.org/JACS

Collagen I Weakly Interacts with the β-Sheets of β_2-Microglobulin and Enhances Conformational Exchange To Induce Amyloid Formation

Cody L. Hoop,[†] Jie Zhu,[†] Shibani Bhattacharya,[‡] Caitlyn A. Tobita,[†] Sheena E. Radford,[*,§] and Jean Baum[*,†]

[†]Department of Chemistry and Chemical Biology, Rutgers University, Piscataway, New Jersey 08854, United States

[‡]New York Structural Biology Center, New York, New York 10027, United States

[§]Astbury Centre for Structural Molecular Biology and School of Molecular and Cellular Biology, Faculty of Biological Sciences, University of Leeds, Leeds LS2 9JT, U.K.

Supporting Information

ABSTRACT: Amyloidogenesis is significant in both protein function and pathology. Amyloid formation of folded, globular proteins is commonly initiated by partial or complete unfolding. However, how this unfolding event is triggered for proteins that are otherwise stable in their native environments is not well understood. The accumulation of the immunoglobulin protein β_2-microglobulin (β_2m) into amyloid plaques in the joints of long-term hemodialysis patients is the hallmark of dialysis-related amyloidosis (DRA). While β_2m does not form amyloid unassisted near neutral pH *in vitro*, the localization of β_2m deposits to joint spaces suggests a role for the local extracellular matrix (ECM) proteins, specifically collagens, in promoting amyloid formation. Indeed, collagen and other ECM components have been observed to facilitate β_2m amyloid formation, but the large size and anisotropy of the complex, combined with the low affinity of these interactions, have limited atomic-level elucidation of the amyloid-promoting mechanism(s) by these molecules. Using solution NMR approaches that uniquely probe weak interactions in large molecular weight complexes, we are able to map the binding interfaces on β_2m for collagen I and detect collagen I-induced μs−ms time-scale dynamics in the β_2m backbone. By combining solution NMR relaxation methods and ^{15}N-dark-state exchange saturation transfer experiments, we propose a model in which weak, multimodal collagen I−β_2m interactions promote exchange with a minor population of amyloid-competent species to induce fibrillogenesis. The results portray the intimate role of the environment in switching an innocuous protein into an amyloid-competent state, rationalizing the localization of amyloid deposits in DRA.

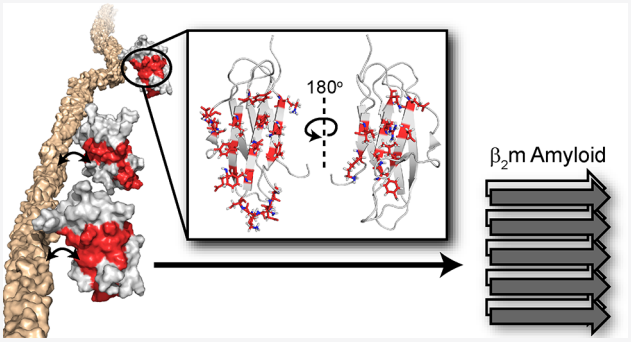

INTRODUCTION

Several proteins self-associate into amyloid fibrils, which in some cases have functional roles,[1−3] but for others are associated with debilitating human diseases[4−6] including Alzheimer's disease, Parkinson's disease, Huntington's disease, type II diabetes, cataracts, and dialysis-related amyloidosis (DRA). The protein precursors of amyloid diseases have unrelated primary sequences and structures,[7] spanning natively unfolded (intrinsically disordered) states, such as α-synuclein, amyloid-β peptide, and tau,[8−10] to stable, globular proteins, such as β_2-microglobulin (β_2m), transthyretin, and immunoglobulin light chains.[11−13] Initiation of amyloid formation of the latter class of proteins requires complete or partial unfolding of monomeric precursors, which can transiently assume amyloid-competent state(s). This kinetic barrier may be lower for intrinsically disordered proteins. However, what triggers the initial unfolding and subsequent amyloidogenesis of natively folded globular proteins remains poorly understood.

Accumulation of β_2m amyloid plaques in the joints of long-term hemodialysis patients leads to DRA and arthritic symptoms.[14−17] In healthy individuals, β_2m dissociates from the major histocompatibility complex-I (MHC-I), is released into the plasma, and is carried to the kidneys for degradation.[18,19] However, when hemodialysis or peritoneal dialysis are required due to kidney failure, β_2m is not efficiently removed from the plasma, leading to increased concentrations of the protein by up to 60-fold.[16,20,21] Remarkably, despite being transported throughout the body, β_2m accumulates into amyloid plaques specifically in skeletal tissues of dialysis patients.[16,21−24] The mechanism(s) by which β_2m fibrillizes *in*

Received: September 26, 2019
Published: December 25, 2019

DOI: 10.1021/jacs.9b10421
J. Am. Chem. Soc. 2020, 142, 1321−1331

vivo is not well understood, since in isolation, the wild-type protein (the major culprit of DRA) resists amyloid formation *in vitro* under physiological conditions, even at high (100 μM) concentrations.[25,26] It has been proposed that β_2m amyloid localized in the joints could result, at least in part, from interactions with the major components of the extracellular matrix (ECM) in bone and cartilage: collagens I and II[20−23] and glycosaminoglycans (GAGs).[27−29] The binding affinities of β_2m to these collagens have been shown to be in the μM−mM range,[30] with preference for collagen I.[27] Although the interaction is weak, it is nonetheless pathologically significant, as images of *ex vivo* DRA plaques reveal β_2m amyloid covering the surface of collagen I fibrils.[21] Indeed, recent kinetic studies have revealed that ECM components, such as collagens[21,28,29] and GAGs[28,29,31,32] as well as preformed fibril seeds and other cofactors,[25,26,28,31−49] induce and modulate β_2m amyloid formation. However, atomic details of how these components interact with, and induce, amyloid formation of β_2m have remained an open question.

The weak nature of the interaction and large, anisotropic shape of the β_2m−collagen I complex creates a challenge for deriving atomic-level information on how collagen I−β_2m interactions initiate β_2m amyloidogenesis. The immunoglobulin fold of monomeric β_2m has dimensions of ∼4 nm × 2 nm × 2 nm, whereas the simplest triple helical unit of collagen I has strikingly larger dimensions of 300 nm × 1.5 nm × 1.5 nm. Collagen I triple helices assemble into even larger, structured fibrils that have diameters ranging from 10−500 nm and lengths on the μm-scale. Collagen I therefore presents as a large surface with numerous reactive groups for β_2m interactions. These challenges are not insurmountable, however, as powerful solution nuclear magnetic resonance (NMR) spectroscopy methods can indirectly probe large, lowly populated complexes in site-specific detail that are invisible by other biophysical techniques.

In this study, by utilizing NMR spectroscopy experiments designed to probe large complexes, we are able to pinpoint the binding interfaces of wild-type β_2m for collagen I at physiological pH and have shown the interfaces to involve both β-sheets of the native protein, suggestive of different binding modes between these two proteins. Residues identified at the binding interface include both hydrophobic and hydrophilic side chains. Through ^{15}N relaxation experiments, we have also found that collagen I increases the number of residues in β_2m involved in conformational exchange on the μs−ms time scale. These regions include residues 6−11 (β-strand A), 36−39 (β-strand C), 51 (β-strand D), and 91−94 (β-strand G) in the edge β-strands and loop residues 15−20 (loop AB), 35 (loop BC), 52−53 (loop DE), 63 (loop DE), and 78 (loop EF), the dynamics and conformations of which are known to be important for β_2m amyloid formation.[31,38,50,51] We propose that the weak interactions of collagen I with the β_2m β-sheets and loops promote exchange of the native protein with minor populations of more amyloid-competent species that induce fibrillogenesis. This study illuminates how a protein component, collagen I, local to the environment in which β_2m plaques are found, can interact with a stable, globular protein to initiate debilitating amyloid formation.

RESULTS

Collagen I Induces β_2m Amyloid Formation in a Concentration-Dependent Manner. Since the direct interaction of β_2m with collagen in the joint space has been proposed to induce β_2m amyloid formation,[21,27] we probed the β_2m−collagen I interaction under physiological pH conditions (pH 7.4) using solid-phase enzyme-linked immunosorbent assays (ELISA) (Figures 1A and S1). This is a colorimetric assay that detects an HRP-conjugated anti-β_2m primary antibody and indicates the presence of β_2m bound to collagen I immobilized in a 96-well plate. Importantly, the results suggest a dose-dependent interaction of the two proteins, consistent with previously published results,[27] under the conditions employed here. We observe that the β_2m−collagen I binding does not easily saturate with increasing concentrations of β_2m (up to 100 μM; Figure S1), consistent with the low affinity of the interaction at pH 7.4 ($K_d \approx 410$ μM)[30] measured previously by surface plasmon resonance. The adhesion of β_2m to casein was monitored as a negative control, for which no significant binding was observed (Figure 1A).

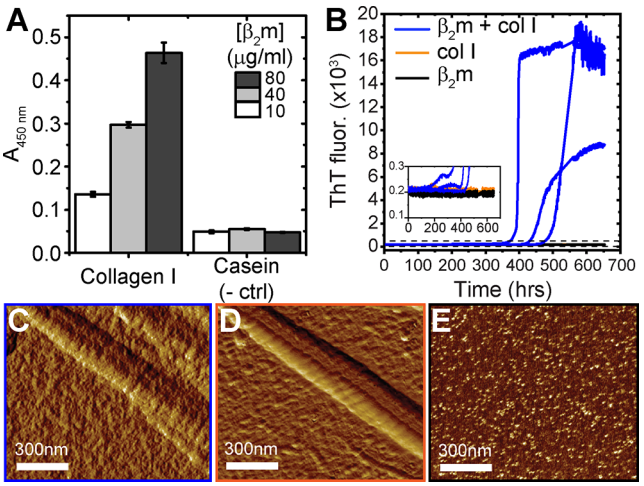

Figure 1. Detection of collagen I-driven β_2m amyloid formation. (A) ELISA probing dose-dependent adhesion of β_2m (10−80 μg/mL) to collagen I (10 μg/mL) or casein (10 μg/mL, used as a negative control), at pH 7.4. The average absorbance at 450 nm from triplicates within the same plate are reported with the standard deviation given as error bars. (B) ThT fluorescence curves of 85 μM β_2m (black), 85 μM β_2m + 3.4 mg/mL (8.5 μM) collagen I (blue), or 3.4 mg/mL collagen I alone (orange) over 650 h in 10 mM sodium phosphate buffer, pH 7.4, shaking at 600 rpm at 37 °C. Three representative curves are given for each condition. The inset shows a zoom-in of the baseline of the ThT fluorescence curves to highlight the lack of fluorescence enhancement for both β_2m (black) and collagen I (orange) alone. (C−E) Representative amplitude-modulated AFM images of (C) β_2m coincubated with collagen I fibrils, (D) collagen I fibrils alone, and (E) β_2m alone after incubation for 96 h at 37 °C with shaking.

Having verified the β_2m−collagen I interaction under physiological pH conditions, we next monitored amyloid growth of β_2m in the presence or absence of collagen I by thioflavin T (ThT) fluorescence (Figure 1B). In the presence of 3.4 mg/mL collagen I (1:0.1 molar ratio β_2m:collagen I), β_2m amyloid is formed within 400−600 h at pH 7.4 (Figure 1B, blue), as evident by enhanced ThT fluorescence. This is not observed in the absence of collagen I in the same conditions, and collagen I alone does not show ThT fluorescence enhancement (Figure 1B). Notably, at lower concentrations of collagen I, lower β_2m concentrations, or

DOI: 10.1021/jacs.9b10421
J. Am. Chem. Soc. 2020, 142, 1321−1331

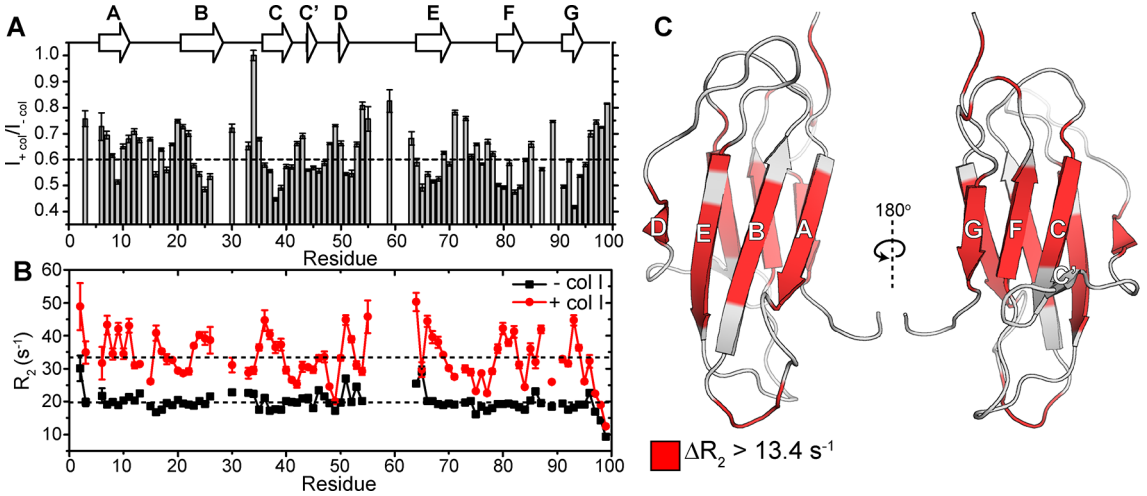

Figure 2. Characterizing residue-specific β_2m−collagen I binding through ^{15}N-R_2 measurements. (A) Amide backbone signal intensity ratios from ^{1}H−^{15}N HSQC spectra of 300 μM β_2m in the presence of 1.2 mg/mL collagen I compared with values in the absence of collagen I (gray bars). The dashed line is drawn at the average signal intensity ratio over the entire protein. Dips in the signal intensity reflect regions maximally perturbed by the presence of collagen I. Error bars are propagated from the noise level of the spectra. The secondary structural elements of β_2m are indicated above the plot. (B) ^{15}N-R_2 measurements of 300 μM β_2m in the presence (red) or absence (black) of 1.2 mg/mL collagen I. The errors are propagated from the fitting errors. The dashed lines indicate the mean ^{15}N-R_2 values of β_2m in the presence or absence of 1.2 mg/mL collagen I over the entire protein. All experiments were conducted in TBS, pH 7.4 containing 0.5 mg/mL casein as a nonspecific binding blocking agent at 10 °C. Note that in these conditions, several residues in the DE loop do not have observable peak intensities in the ^{1}H−^{15}N HSQC spectrum due to inherent conformational exchange, consistent with previous results.[49] (C) Solution NMR structure of the WT-β_2m monomer (PDB: 2XKS)[49] highlighting residues that show an increase in ^{15}N-R_2 higher than 13.4 s^{-1} (the mean Δ^{15}N-R_2) upon addition of 1.2 mg/mL collagen I.

shorter time scales, fibrils are not observed.[29,31] Collagen I-induced β_2m amyloid formation is accelerated at pH 6.2 relative to at pH 7.4 (Figure S2A,B), enabling measurement of the dependence of the rate of fibril formation on the concentration of collagen I. The results showed that at this pH, β_2m amyloid formation is dependent on collagen I concentration, as addition of 3.4 mg/mL collagen I significantly reduces the lag time and half time of β_2m aggregation relative to 0.34 or 0.17 mg/mL collagen I (Figure S2C,D). This trend is consistent with our previously published data,[29] in which increasing concentrations of collagen I (0−0.47 mg/mL) accelerated β_2m amyloid formation at pH 6.2 in the presence of a constant concentration of the glycosaminoglycan, heparin. These results reinforce earlier proposals that collagen I−β_2m interactions play a significant role in triggering β_2m fibril formation.[21] Atomic force microscopy (AFM) images also showed that β_2m interacts with collagen I fibrils, consistent with previous results,[21] showing that β_2m coats the collagen I fibril surface before detectable fibril formation occurs (monitored by ThT fluorescence), obscuring the characteristic collagen I fibril D-banding that is clearly observed in the absence of β_2m (Figure 1C,D). Importantly, control experiments showed that β_2m alone (Figure 1E) does not aggregate in the conditions employed, with no fibrils or high molecular weight assemblies observed by AFM. Together, these data confirm that adhesion of collagen I and β_2m induces amyloid formation under physiological conditions *in vitro*, while β_2m is not able to form amyloid within these time scales *in vitro* in the absence of collagen I.

Weak, but Specific β_2m−Collagen I Interactions Observed through ^{15}N-R_2 Perturbations. In order to understand the mechanistic details by which collagen I interacts with β_2m and initiates amyloid formation, we used solution NMR methods, which provide an excellent toolbox of approaches able to characterize residue-specific features of weak protein−protein interactions on multiple time scales.[52−55] A titration of collagen I into a β_2m monomer solution showed no significant chemical shift perturbations in ^{1}H−^{15}N heteronuclear single quantum correlation (HSQC) spectra (Figure S3). However, a residue-specific attenuation of the peak intensities was observed with increasing collagen I concentrations (Figure 2A), suggesting specific, although weak, β_2m−collagen I interactions. To minimize collagen I aggregation during the NMR experiments and to capture the most specific interactions, we proceeded with low collagen I concentrations (0.6−1.2 mg/mL) that displayed consistent residue-specific perturbations and kept samples at 10 °C, allowing NMR spectra to be acquired for over 1 week without visible alterations in spectral quality. Under these conditions, addition of 1.2 mg/mL collagen I to 300 μM β_2m resulted in a reduction in resonance intensity of all peaks, consistent with transient formation of a high molecular weight complex (Figure 2A). However, the greatest reduction in peak intensities occurred for residues in the eight β-strands of the wild-type protein (Figure 2A). These peak intensity losses arise, in part, from increased ^{15}N-transverse relaxation rates (R_2), which are sensitive to changes in internal motions on the ps−ns time scale and conformational exchange on the μs−ms time scale. Indeed, at these concentrations, we observe an overall increase in ^{15}N-R_2 values of β_2m relative to their magnitude in the absence of collagen I, but importantly, the increase is not uniform across all residues, but is residue specific, involving predominantly residues 2−3 (N-terminus), 7−11 (β-strand A), 16−19 (loop AB), 23−26 (β-strand B), 35−39 (β-strand C), 50−52 (β-strand D), 64, 66−69 (β-strand E), 79−82 (β-strand F), 85, 87 (loop FG), and 91−94 (C-terminal β-strand G) (Figure 2B,C). The increased ^{15}N-R_2 at these specific sites could have multiple origins, arising from reduced backbone mobility upon direct interaction with collagen I and/or to line broadening due to exchange between

DOI: 10.1021/jacs.9b10421
J. Am. Chem. Soc. 2020, 142, 1321−1331

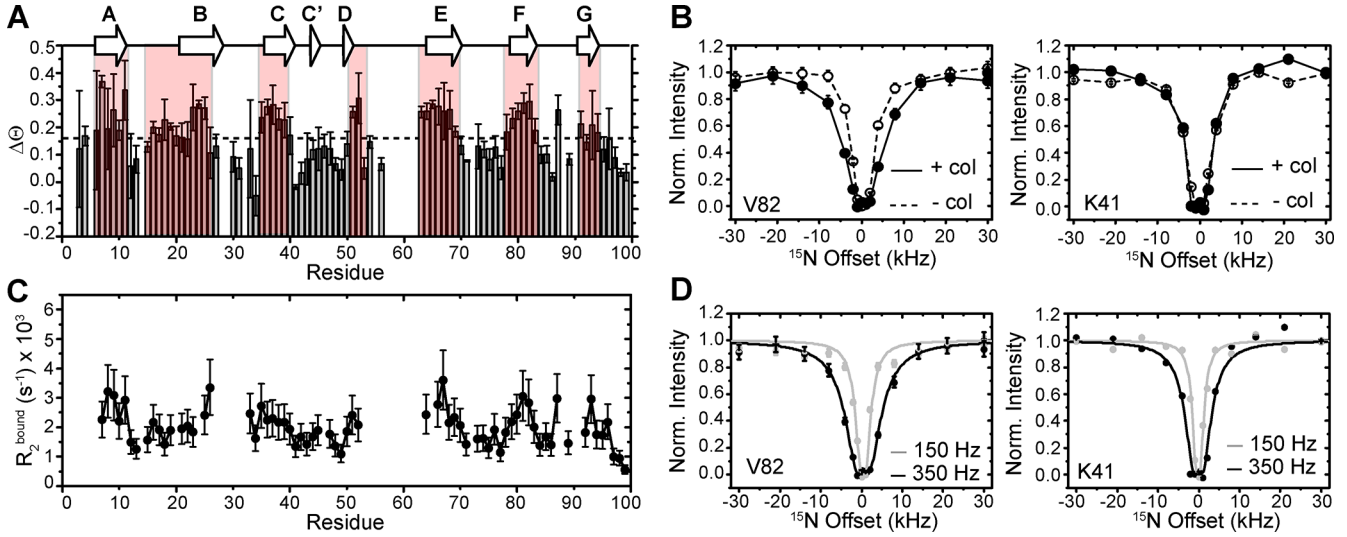

Figure 3. ^{15}N-DEST to identify collagen-binding interface on ^{15}N-β_2m. (A) $\Delta\Theta$ calculated from ^{15}N-β_2m DEST intensities at ±30 kHz and ±4 kHz ^{15}N offsets with a 350 Hz saturation frequency in the presence or absence of collagen I (gray bars). The secondary structure is shown above the plot. (B) Examples of ^{15}N-DEST profiles of 300 μM ^{15}N-β_2m in the presence (solid line, solid circles) or absence (dashed line, open circles) of 0.6 mg/mL collagen I. V82 in β-strand F shows enhancement of the DEST effect upon addition of collagen, whereas K41 in the C−C′ loop does not. (C) ^{15}N-R_2^{bound} for each residue determined from fitting ^{15}N-DEST profiles to the McConnell equations. (D) Examples of fit DEST profiles using the same residues as in (B). Data points are shown as circles and the fits as solid lines (gray, 150 Hz saturation; black, 350 Hz saturation). All experiments were carried out in TBS, pH 7.4, 10 °C at 700 MHz ^{1}H Larmor frequency.

species with different chemical shifts, especially since the observed ^{15}N-ΔR_2 is dependent on magnetic field (700 MHz vs 900 MHz, Figure S4). In order to disentangle these contributions to the increase in ^{15}N-R_2, we proceeded with two sets of NMR experiments: ^{15}N-dark-state exchange saturation transfer (DEST) experiments, which can identify residues in β_2m interacting with the large collagen I fibrils and in-phase Hahn-echo experiments, which detect conformational exchange on the μs−ms time scale.

Pinpointing the Collagen I Interaction Interface on β_2m through ^{15}N-DEST. In order to determine which residues of β_2m interact most intimately with collagen I, we used ^{15}N-DEST experiments.[56,57] This experiment is optimal when there is a measurable increase in R_2 due to formation of a transient, large molecular weight complex that is NMR-invisible because of its high R_2 and detects the exchange between an observable "light" state (free monomeric β_2m) and the NMR-invisible "dark" state (the high molecular weight collagen I−β_2m complex). In the DEST experiment, resonances of high molecular weight species with high R_2 values, such as the collagen I−β_2m complex, can be partially saturated by weak radiofrequency (RF) fields at frequency offsets far from monomeric β_2m resonances. Saturation transfer to the observable monomeric species by chemical exchange is detected as a loss in monomeric β_2m signal intensity. The broadening of these DEST saturation profiles (reduced signal intensities at further frequency offsets) in the presence of collagen I, relative to in its absence, is therefore indicative of residues at the interaction interface (Figure 3A,B). The "broadness" of the profiles was measured by calculating the DEST difference (Θ) for each residue, which is a measure of the relative effects of on-resonance and off-resonance ^{15}N saturation. Using a saturation frequency of 350 Hz, we measured Θ as $\Theta = \frac{(I_{30kHz} + I_{-30kHz}) - (I_{4kHz} + I_{-4kHz})}{(I_{30kHz} + I_{-30kHz})}$, where ±30 kHz were the most off-resonance ^{15}N offsets, and ^{15}N offsets of ±4 kHz provide enough saturation transfer from bound to unbound β_2m to show significant intensity loss without eliminating the signal in most cases. Notably, we observe that the broadening of the DEST saturation profiles is residue-specific and not uniform across all β_2m residues, with some residues showing no change in the DEST difference in the presence of collagen I (Figure 3A,B). Examples of DEST profiles in the presence or absence of collagen I for a residue that shows DEST due to collagen I binding (V82 in β-strand F) and one that does not (K41 in the C−C′ loop) are given in Figure 3B. In Figure 3A, those residues with $\Delta\Theta$ larger than the mean, and likely have the most direct contacts with the collagen in the β_2m−collagen I complex (shaded red), include residues 6−11 (β-strand A), 15−20 (loop AB), 21−26 (β-strand B), 35 (loop BC), 36−39 (β-strand C), 51 (β-strand D), 52−53 (loop DE), 63 (loop DE), 64−69 (β-strand E), 78 (loop EF), 79−83 (β-strand F), and 91−94 (β-strand G).

In addition, the full DEST profiles can be used to quantify residue-specific transverse relaxation values of β_2m in the collagen I-bound state (R_2^{bound}) and exchange kinetics between the bound and unbound β_2m. Since the ΔR_2 may be due to more complex processes than collagen I binding alone, such as an overall increased viscosity due to the presence of the large collagen I molecules, we fit only the ^{15}N DEST profiles of each residue with 150 and 350 Hz RF saturation to the McConnell equations.[56,57] The use of two RF fields provides an additional constraint to distinguish between models with equal fits to data acquired at only one RF field and provides more accurate determination of kinetic parameters.[57] Fitting to a simple two-state model, the population of the unbound, monomeric β_2m was determined to be 94 ± 2% with an apparent first-order rate constant for the conversion of β_2m from unbound to collagen I-bound conformation (k_{on}^{app}) of 6.4 ± 0.8 s^{-1}. We interpret the direct binding interface to be the residues with the highest R_2^{bound}. The ^{15}N-R_2^{bound} profile shows a similar trend to the $\Delta\Theta$ profile (Figure 3A,C) and suggests that binding interfaces for collagen I on β_2m occur on both β-sheets. Examples of fitting to the experimental values of residues V82 (in a binding

DOI: 10.1021/jacs.9b10421
J. Am. Chem. Soc. 2020, 142, 1321−1331

region) and K41 (away from interface) are shown in Figure 3D.

Collagen I-Induced Conformational Exchange in β_2m Revealed by ^{15}N Relaxation. The enhanced observed ^{15}N-R_2 of β_2m may not only be due to the increased intrinsic ^{15}N-R_2 caused by slowed molecular motions upon binding with a high molecular weight species (such as in a large complex) but also to an increased contribution of chemical exchange dynamics on the μs−ms time scale, since the ^{15}N-ΔR_2 is dependent on the magnetic field (Figure S4). Chemical exchange describes the interconversion of a residue between multiple states with distinct chemical shifts, such as in the case of conformational conversion or complex formation. In order to qualitatively determine which residues in β_2m are in conformational exchange in the presence of collagen I, we use ^{15}N in-phase Hahn echo experiments (R_2^{HE}) to estimate the chemical exchange contribution to the observed ^{15}N-R_2, denoted R_{ex}. An increase in R_{ex} in the presence of collagen I, relative to in its absence, suggests collagen I-induced conformational exchange on a per residue basis. At pH 7.4 and 10 °C, few residues in β_2m have R_{ex} values >10 s^{-1} in the absence of collagen I as measured by the in-phase Hahn echo experiments (Figure 4A). In the absence of collagen I, the N-terminal seven amino acids and residues in the BC and DE loops (for which several signals are unobservable) are inherently in conformational exchange (Figure 4A). Upon addition of 0.6 mg/mL collagen I, the regions with high R_{ex} are expanded to include the N-terminus and full β-strand A, part of β-strand B to part of β-strand C, including the connecting BC loop, β-strand D, the DE loop, the C-terminal residue of β-strand F into the FG loop, and the C-terminal β-strand G (Figure 4B). Conformational dynamics in specific regions of β_2m, including the N-terminal region, edge β-strands C and D, and the BC loop that contains *cis* Pro32, have been shown previously to be crucial in controlling the amyloidogenicity of the protein.[49,58−60] Thus, the enhanced conformational exchange induced by the presence of collagen I may facilitate minor populations of amyloid-component states of β_2m.

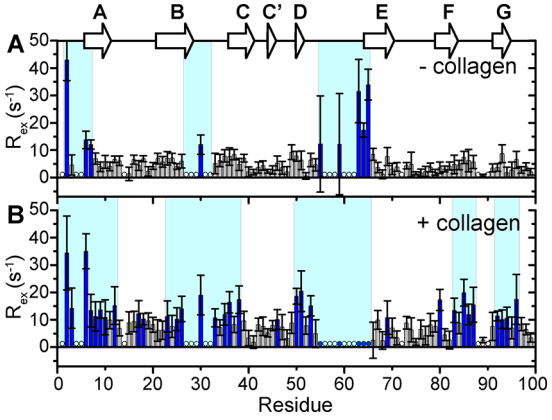

Figure 4. Conformational exchange in β_2m induced by collagen I. Relaxation exchange rates (R_{ex}) obtained by ^{15}N-R_2 Hahn echo experiments for each residue in 300 μM ^{15}N-β_2m in the absence (A) or presence (B) of 0.6 mg/mL collagen I at pH 7.4, 10 °C, 700 MHz ^{1}H Larmor frequency. R_{ex} values over 10 s^{-1} are indicated in blue bars. Regions shaded in cyan in both panels contain several residues with R_{ex} > 10 s^{-1} in the respective conditions. Residues with unobservable cross-peaks in the absence of collagen I are indicated by open circles. Residues that are observable in the absence of collagen I, but are reduced to the level of the noise in the presence of collagen I are indicated by filled blue circles. Error bars are propagated from fitting errors.

DISCUSSION

A Novel Collagen I Binding Surface on β_2m. Amyloid formation of β_2m at physiological pH *in vitro* requires assistance by cofactors.[21,25,26,28,29,31−49] In particular, ECM molecules, such as collagens and GAGs, have been targeted as amyloid-inducing cofactors, since β_2m amyloid formation is localized to musculoskeletal tissues.[16,22−24] While previous experiments have focused on the kinetics of amyloid formation in the presence of these molecules,[21,28,29,31,61] a detailed atomistic description of the interactions involved and how these may enhance β_2m conformational dynamics and amyloid formation had not been elucidated. Here, we have used complementary NMR relaxation-based experiments to pinpoint residues of β_2m involved in the collagen I binding interface and collagen I-induced dynamics that lead to enhanced β_2m amyloid formation at neutral pH *in vitro*. The ^{15}N-DEST experiments indicate that residues in β-strands A, B, C, D, E, F, and G form interaction surfaces with collagen I. These provide two surfaces of mixed hydrophilic and hydrophobic composition (Figure S5). Both contain hydrophobic patches, with the ABED β-sheet displaying several aromatic residues on the interaction surface (Figure S5). Since both β-sheets on opposite sides of β_2m were shown to interact with the collagen I surface, binding must be multimodal involving interaction surfaces formed by K6, Q8, Y10, F22, N24, Y26, S52, Y63, L65, Y67, and E69 on the ABED β-sheet and E36, D38, L40, A79, R81, N83, I92, and K94 on the GFC β-sheet (Figures 3 and S5). Comparison of the molecular dimensions of the interacting molecules (4 nm × 2 nm × 2 nm for β_2m, 300 nm × 1.5 nm for a collagen I triple helix, and microns in length and up to 500 nm in diameter for mature collagen I fibrils) highlights the potential for a myriad of binding modes, enabling independent binding of several β_2m molecules to the same collagen molecule (Figure 5A,B). Importantly, the collagen I triple helix surface is interspersed with numerous hydrophilic and hydrophobic residues along its length (Figure 5A). The collagen I fibril surface maintains this repeating pattern of surface chemistries (Figure 5B), enhancing the potential for multiple binding modes to complementary surfaces on β_2m (Figure 5C).

Collagen I is known to interact with multiple immunoglobulin-like protein folds through binding interfaces that include both hydrophobic and hydrophilic residues. Interactions of collagen I with osteoclast-associated receptor (OSCAR), leukocyte-associated immunoglobulin-like receptor-1 (LAIR-1), and glycoprotein VI (GPVI) play functional roles in immune system regulation[63−66] and platelet activation.[67−69] Similar to the β-sheet binding interface on β_2m for collagen I identified here, the collagen I binding sites on OSCAR and LAIR-1 are also found in β-sheet regions.[70,71] In the case of the OSCAR−collagen I interactions, Tyr and Arg residues that line the interacting β-sheet of OSCAR have been suggested to play a primary role.[70] LAIR-1 binds primarily to collagen fragments rich in Gly, Pro, and hydroxyproline (GPO) content, but also has been shown to interact with multiple binding motifs in collagen II and III toolkit peptides, some of which are not GPO rich.[71] NMR and mutagenesis studies on LAIR-1 have shown that depletion of Arg or Glu at the putative β-sheet interface showed decreased collagen binding, suggesting a role

DOI: 10.1021/jacs.9b10421
J. Am. Chem. Soc. 2020, 142, 1321−1331

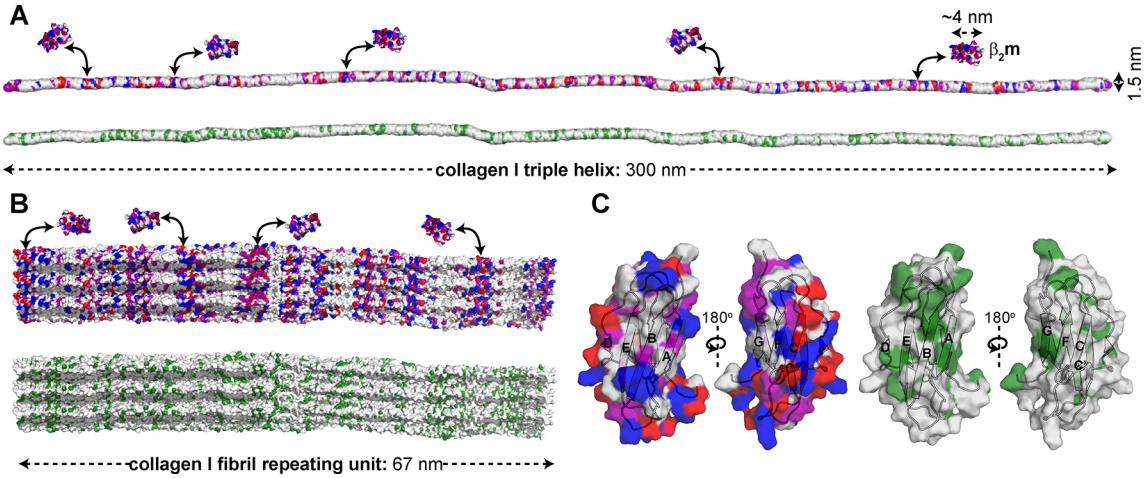

Figure 5. Potential surface contacts for β_2m−collagen I interaction. (A) Surface model of the collagen I monomer (PDB: 3HR2)[62] color-coded by amino acid type (top, hydrophilic; bottom, hydrophobic). A surface representation of β_2m is shown for size comparison (PDB: 2XKS).[49] As an example, electrostatic surfaces of β_2m are shown weakly interacting with electrostatic surfaces of collagen I. (B) Surface models of the collagen I fibril repeating unit (built from PDB: 3HR2),[62] color-coded by amino acid type (top, hydrophilic; bottom, hydrophobic). The repeating unit is ∼67 nm in length, however mature fibrils can be microns long and ∼500 nm in diameter. Distinct bands of electrostatic residues are observed within the repeating unit. (C) Surface representation of β_2m monomer (PDB: 2XKS)[49] color-coded by amino acid type (left, hydrophilic; right, hydrophobic). All models are color-coded as red, acidic; blue, basic; purple, uncharged-polar; and green, hydrophobic.

for electrostatic interactions.[72] GPVI also recognizes GPO-rich collagen motifs, however through a unique hydrophobic groove formed by a β-strand connecting loop that is flanked by hydrophilic residues.[73−75] Thus, although these proteins all share a similar immunoglobulin fold, each shows a unique binding interface to collagen, interacting in grooves formed by β-sheets or loops and having both hydrophobic and hydrophilic residues that each plays fundamental roles in binding.

Collagen-Induced Conformational Dynamics in β_2m Reflect Amyloid Prone Dynamics. Beyond the structured collagen I-binding interface of β_2m, using ^{15}N relaxation experiments, we observe enhanced dynamics in the N- and C-terminal regions, the BC and FG loops, and the β-strand D of β_2m upon complex formation. Enhanced dynamics in each of these regions has been proposed to play key roles in the aggregation mechanism of wild-type β_2m.[38,49−51,59,60,76−86] Amyloid formation of β_2m is nucleation dependent and proceeds through a near native folding intermediate, I_T, that is in part defined by a non-native *trans*-His31-Pro32 peptide bond in the BC loop.[38,50,51,87,88] NMR studies of a P32G-β_2m variant, which inherently has a *trans*-His31-Gly32 peptide bond, showed significant line broadening in β-strands A and D and the BC and FG loops relative to WT-β_2m.[38] This was interpreted to result from conformational conversion between the native and I_T conformations.[38] The observation of increased R_{ex} of these same regions upon addition of collagen I to WT-β_2m in this study is consistent with the same regions undergoing conformational exchange from the native state to enhance the formation of non-native species with enhanced amyloid potential.

The *cis*−*trans* isomerization of Pro32 is aided by displacement of the N-terminal six residues, as in the naturally occurring amyloidogenic variant, ΔN6,[49,76,89,90] which destabilizes the protein, allowing β_2m to sample multiple amyloidogenic conformations that enhance the rate of aggregation.[38,50,51,76,81−83,87,88] In addition, NMR relaxation experiments show enhanced dynamics in β-strand D and the BC and DE loops of amyloidogenic ΔN6, which have been proposed to contribute to its higher aggregation propensity.[49] Consistent with this, collagen I-induced enhancement of conformational exchange in the BC and DE loops of WT-β_2m in this work may rationalize the increased β_2m amyloidogenicity in the presence of collagen I.

Another proposed mechanism of the initiation of aggregation of WT-β_2m involves destabilization of the edge β-strands A, D, C, and G to expose the β-strands with the highest aggregation propensity, namely β-strands B and E, unleashing their amyloid potential. Protection of the aggregation-prone β-strands was suggested to play a role in the amyloidogenicity of pathological variant D76N-β_2m, which rapidly self-assembles into amyloid fibrils at neutral pH *in vitro* in the absence of cofactors,[59] and an aggregation-resistant variant, W60G-β_2m.[60] Indeed, a recent study on D76N-β_2m proposed that the enhanced aggregation propensity of this protein arises, in part, due to destabilization of the edge strands and conformational exchange in β-strand A, the BC loop, and the EF loop.[59] In line with this hypothesis, reduced aggregation propensity of W60G-β_2m, relative to WT-β_2m, has been suggested to result from increased protection of the solvent exposed residues in the aggregation-prone β-strands, along with reduced dynamics of the protein, including in edge β-strands and the aggregation-prone β-strand B.[60] Analogously, we find that collagen I enhances conformational exchange in the edge β-strands, A, D, C, and G, which may allow increased sampling of alternative conformations in these strands, deprotecting the aggregation-prone β-strands B and E, to enhance amyloidogenicity.

A Proposed Mechanism of Collagen I-Driven β_2m Amyloidogenesis. With the new insights into the binding interface of collagen I on β_2m and its impact on β_2m dynamics described here, we propose a mechanistic view by which collagen I might drive amyloidogenesis of β_2m (Figure 6). In the presence of collagen I, the β-sheets of β_2m are available for binding to the collagen I surface, with both β-sheets providing potential binding interfaces, indicative of multiple binding modes, rather than a unique and specific binding interface. Through modification of the dynamics of β_2m in the BC loop and the edge strand regions, concomitant sampling of amyloid-competent species, including the I_T state,[87,88] may be increased

DOI: 10.1021/jacs.9b10421
J. Am. Chem. Soc. 2020, 142, 1321−1331

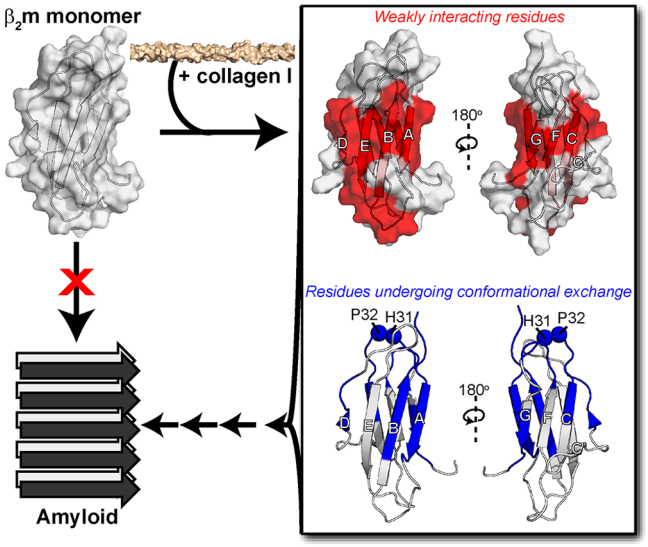

Figure 6. Proposed mechanism for collagen-driven β_2m amyloidogenesis. Alone, the β_2m monomer (PDB: 2XKS)[49] does not readily aggregate into amyloid fibrils. Upon addition of collagen I, we have observed interaction interfaces to include both β-sheets of β_2m through the ^{15}N-DEST experiment (red). Collagen also induces conformational exchange in regions colored in blue, as assessed by ^{15}N relaxation experiments. The interaction of collagen I with the structured regions of β_2m enhances conformational exchange, promoting formation of amyloid-competent species and inducing aggregation.

by a heightened probability of *cis*–*trans* isomerization of Pro32[38,50,51] and/or exposure of highly amyloidogenic B and E β-strands, enabling them to realize their amyloid potential. Binding to collagen I may also concentrate bound β_2m molecules, enhancing the probability of self-association, or may increase the potential for secondary nucleation on the collagen I surface, enhancing fibril formation. All, or several, of these mechanisms may be at play to catalyze β_2m aggregation both *in vitro* and provide a molecular rationale for the deposition of β_2m in collagenous-rich joints in dialysis patients.[16,21−24] More generally, they also serve as an exemplar of the key role of the physiological environment in amyloid formation, by rationalizing the often remarkably specific deposition of amyloid to different tissues,[1] and in some cases, of different variants of the same protein in different tissues.[91,92] The methods used here to interrogate the weak-transient interaction of the large, β_2m–collagen I complex can be extended to future studies to gain atomic-level insight into how other physiologically relevant cofactors promote amyloid formation of globular proteins involved in other amyloid diseases.

MATERIALS AND METHODS

Expression and Purification of β_2m. Wild-type β_2m was expressed recombinantly in *Escherichia coli* BL21(DE3) pLysS cells by induction with 1 mM IPTG overnight at 37 °C, following methods described previously.[39] Cells were lysed in 25 mM Tris-HCl buffer, pH 8.0 and with an Avestin Emulsiflex-C5 homogenizer. β_2m is accumulated in inclusion bodies. To extract the β_2m from inclusion bodies, the cell pellet was washed five times with 25 mM Tris-HCl buffer, pH 8.0 and solubilized in 25 mM Tris-HCl, pH 8.0 buffer containing 8 M urea, rocking overnight at room temperature. The protein was verified to be in the soluble fraction by SDS-PAGE. β_2m was refolded by dialyzing against 25 mM Tris-HCl buffer, pH 8.0 at 4 °C and purified by anion exchange (HiTrap Q HP, GE Healthcare). The protein was further purified by size exclusion chromatography with a HiLoad 26/600 Superdex 75 gel filtration column (GE Life Sciences). Protein purity was verified by SDS-PAGE, and concentrations for experiments were determined by measuring the absorbance at 280 nm using a molar extinction coefficient of 19,060 M^{-1} cm^{-1}. [U−^{15}N]-enriched β_2m was expressed recombinantly for NMR using the same protocol in HCDM1 minimal media supplemented with ^{15}N-ammonium chloride.

ELISA. Relative adhesion of variable concentrations of β_2m to collagen I was determined by ELISA experiments. Nunc Maxisorp 96-well plates (Thermo Scientific) were coated with 100 μL of collagen I from rat tail tendon (BD Biosciences; 10 μg/mL in 10 mM acetic acid) overnight at 4 °C. Uncoated areas on the plates were blocked with 200 μL of 0.5% w/v casein in binding buffer at room temperature for 1 h. The binding and washing buffer consisted of PBS at pH 7.4 with 0.05% v/v Tween 20 (PBS-T) and 0.05% w/v casein as a nonspecific blocking agent. After washing the wells three times with 200 μL washing buffer, 100 μL β_2m (10 μg/mL, 40 μg/mL, or 80 μg/mL) in PBS-T and 0.05% w/v casein was added to the wells and incubated for 1 h at room temperature. For the dose-dependent β_2m–collagen I binding curve in Figure S1, β_2m concentrations of 1, 10.5, 21.6, 33.2, 45.6, 58.6, 72.4, and 91.7 μM were used. After three washes with 200 μL washing buffer, 100 μL mouse anti-β_2m monoclonal antibody (1:2000 v/v in PBS-T and 0.05% w/v casein, Millipore Sigma) was bound to β_2m in each well by incubating at room temperature for 1 h. Subsequently, following three washes with 200 μL washing buffer, 100 μL of goat HRP-conjugated antimouse secondary antibody (1:5000 v/v dilution in PBS-T and 0.05% w/v casein, Genscript) was incubated in the wells at room temperature for 30 min. After washing for a final four times with 200 μL washing buffer, the binding of β_2m to collagen I was detected through a colorimetric assay using a 3,3′,5,5′-tetramethylbenzidine substrate kit (Pierce) according to the manufacturer's protocol and measuring the absorbance at 450 nm using a Tecan Infinite F50 plate reader with Magellan software.

ThT Fluorescence. Amyloid fibril formation was monitored by ThT fluorescence assays of β_2m in the presence or absence of collagen I fibrils. Purified recombinant β_2m lyophilized powder was dissolved in 100 μL of 10 mM sodium phosphate buffer, pH 7.4 or pH 6.2 to 1 mg/mL (85 μM). Varying concentrations of collagen I fibrils were separately prepared by incubating collagen I (3.4 mg/mL, 0.34 mg/mL, or 0.17 mg/mL; BD Biosciences) in 100 μL PBS, pH 7.4 at 37 °C for 1 h. Each 100 μL fibril suspension was sonicated in a bath sonicator for 10 min and centrifuged at 16,500 rpm for 10 min to isolate fibrils. Each collagen I fibril pellet was resuspended in 100 μL of 10 mM sodium phosphate buffer, pH 7.4 or pH 6.2 in the presence or absence of 1 mg/mL β_2m. Three to six samples were prepared for each condition and were transferred to a 96-well plate. ThT was added to each sample to a final concentration of 10 μM. ThT fluorescence was monitored over 650 h at 37 °C with shaking at 600 rpm in a POLARstar Omega fluorimeter (BMG Labtech).

NMR. For all NMR experiments, purified recombinant [U−^{15}N]-labeled β_2m was diluted to 300 μM in TBS, pH 7.4 with 0.5 mg/mL casein and 10% v/v D_2O. Before mixing, collagen I from rat tail tendon was dialyzed against TBS, pH 7.4. The concentration of collagen I after dialysis was determined by bicinchoninic acid assay (Pierce). All experiments were performed at 10 °C. All data were collected on 700 MHz Bruker AVIII or 900 MHz AVI NMR spectrometers equipped with TCI-cryo-probes. Data were processed in NMRPipe[93] and analyzed in Sparky.[94]

^{1}H–^{15}N HSQC Spectra. ^{1}H–^{15}N HSQC spectra[95,96] of [U−^{15}N]-labeled β_2m were acquired with different concentrations of collagen I (0, 0.12 mg/mL, and 1.2 mg/mL) in TBS, pH 7.4 with 0.5 mg/mL casein and 10% D_2O at 10 °C. The intensity ratio is taken as the intensity of a given cross-peak in the ^{1}H–^{15}N HSQC spectrum of β_2m in the presence of collagen I relative to the intensity of the same cross-peak in the absence of collagen I, determined in Sparky.[94] The errors were propagated from the signal-to-noise ratios.

^{15}N-R_2 and ^{15}N-R_2^{HE}. [U−^{15}N]-labeled β_2m ^{15}N transverse relaxation rates (R_2) were measured from a series of HSQC-based

DOI: 10.1021/jacs.9b10421
J. Am. Chem. Soc. 2020, 142, 1321−1331

2D $^{1}H-^{15}N$ spectra using the Carr–Purcell–Meiboom–Gill pulse sequence[97] with varying relaxation delays: in the absence of collagen I at 700 MHz- 0, 16, 16, 32, 48, 64, 64, 80, 96, and 112 ms and 900 MHz- 0, 16, 32, 32, 32, 48, 64, 80, 96, 112, and 128 ms and in the presence of 1.2 mg/mL collagen I at 700 mHz- 0, 16, 16, 32, 48, 48, 64, and 80 ms and at 900 MHz- 0, 16, 32, 32, 32, 48, 64, 80, and 96 ms. Relaxation delays used to quantify ^{15}N-R_2 rates of β_2m in the presence of 0.6 mg/mL collagen I at 700 MHz were: 0, 8, 8, 16, 24, 32, and 56 ms and in the absence of collagen I: 0, 8, 8, 16, 24, 40, and 56 ms. ^{15}N-R_2^{HE} informs on the chemical exchange contribution to R_2 by using an in-phase Hahn echo experiment.[98] Relaxation delays used in the R_2^{HE} experiment both in the presence and absence of 0.6 mg/mL collagen I were: 0.768, 7.68, 7.68, 15.4, 23, 38.5, and 61.4 ms. In each case, the R_2 rates were determined by fitting peak intensities to a single exponential decay function. The chemical exchange contribution (R_{ex}) for each β_2m residue in the absence and presence of 0.6 mg/mL collagen I was determined as $R_{ex} = R_2^{HE} - R_2$.

DEST Experiments. The ^{15}N-DEST experiment[56,57] was applied to [U–^{15}N]-labeled β_2m in the presence or absence of 0.6 mg/mL collagen I. In this experiment, an ^{15}N saturation pulse of 150 or 350 Hz was applied for 0.9 ms at different ^{15}N frequency offsets: 0, ±1, ±2, ±4, ±8, ±14, ±21, and ±30 kHz. An experiment in which the ^{15}N saturation pulse was set to 0 Hz with an offset of 30 kHz was also included as a reference. The ^{15}N-DEST profiles were extracted for each residue as the peak intensity at each ^{15}N saturation offset and were fitted to a two-state model using the destfit program[56,57] by Clore and co-workers to obtain R_2^{bound}, p_{bound}, and k_{on}^{app}. The $\Delta\Theta$ profile was obtained by measuring Θ for each β_2m residue in the presence and absence of 0.6 mg/mL collagen I as $\Theta = \frac{(I_{30kHz} + I_{-30kHz}) - (I_{4kHz} + I_{-4kHz})}{(I_{30kHz} + I_{-30kHz})}$ and taking $\Delta\Theta = \Theta_{+col} - \Theta_{-col}$.

■ ASSOCIATED CONTENT

Supporting Information

The Supporting Information is available free of charge at https://pubs.acs.org/doi/10.1021/jacs.9b10421.

Figures that show weak, dose-dependent binding of β_2m to collagen I by ELISA (Figure S1); ThT fluorescence experiments to assess the pH and collagen I concentration dependence of β_2m amyloid formation (Figure S2); an overlay of $^{1}H-^{15}N$ HSQC spectra of [U–^{15}N]-β_2m in the presence of 0 mg/mL, 0.12 mg/mL, or 1.2 mg/mL collagen I (Figure S3); ^{15}N-R_2 measurements of [U–^{15}N]-β_2m in the absence or presence of collagen I at 700 or 900 MHz (Figure S4); and a model showing the amino acid composition of the interacting β_2m β-sheets (Figure S5) (PDF)

■ AUTHOR INFORMATION

Corresponding Authors

*jean.baum@rutgers.edu
*s.e.radford@leeds.ac.uk

ORCID

Cody L. Hoop: 0000-0003-4441-8321
Jie Zhu: 0000-0003-0651-4064

Funding

This work was supported by American Heart Association Postdoctoral Fellowship 17POST33410326 to C.L.H. and NIH grant GM045302 to J.B. Additional support was provided by the Wellcome Trust (204963 and 092896) and the European Research Council (ERC) under European Union's Seventh Framework Programme (FP7/2007–2013) ERC grant agreement no. 322408 to S.E.R. Some of the work presented here was conducted at the Center on Macromolecular Dynamics by NMR Spectroscopy located at the New York Structural Biology Center, supported by a grant from the NIH NIGMS (P41 GM118302) and ORIP/NIH facility improvement grant CO6RR015495. The 900 MHz NMR spectrometers were purchased with funds from NIH grant P41 GM066354, the Keck Foundation, New York State Assembly, and U.S. Department of Defense.

Notes

The authors declare no competing financial interest.

■ ACKNOWLEDGMENTS

We acknowledge Arthur Palmer for helpful discussions. We also acknowledge with thanks the many discussions with our group members. We thank Ana Monica Nunes for contributions in the beginning of this project and Nuria Benseny-Cases, who provided critical insights in the early stages of the work.

■ REFERENCES

(1) Chiti, F.; Dobson, C. M. Protein misfolding, functional amyloid, and human disease. *Annu. Rev. Biochem.* **2006**, *75*, 333–66.
(2) Pham, C. L.; Kwan, A. H.; Sunde, M. Functional amyloid: widespread in Nature, diverse in purpose. *Essays Biochem.* **2014**, *56*, 207–19.
(3) Fowler, D. M.; Koulov, A. V.; Balch, W. E.; Kelly, J. W. Functional amyloid - from bacteria to humans. *Trends Biochem. Sci.* **2007**, *32* (5), 217–224.
(4) Iadanza, M. G.; Jackson, M. P.; Hewitt, E. W.; Ranson, N. A.; Radford, S. E. A new era for understanding amyloid structures and disease. *Nat. Rev. Mol. Cell Biol.* **2018**, *19* (12), 755–773.
(5) Knowles, T. P.; Vendruscolo, M.; Dobson, C. M. The amyloid state and its association with protein misfolding diseases. *Nat. Rev. Mol. Cell Biol.* **2014**, *15* (6), 384–96.
(6) Chiti, F.; Dobson, C. M. Protein Misfolding, Amyloid Formation, and Human Disease: A Summary of Progress Over the Last Decade. *Annu. Rev. Biochem.* **2017**, *86*, 27–68.
(7) Eisenberg, D. S.; Sawaya, M. R. Structural Studies of Amyloid Proteins at the Molecular Level. *Annu. Rev. Biochem.* **2017**, *86*, 69–95.
(8) Nizynski, B.; Dzwolak, W.; Nieznanski, K. Amyloidogenesis of Tau protein. *Protein Sci.* **2017**, *26* (11), 2126–2150.
(9) Korsak, M.; Kozyreva, T. Beta Amyloid Hallmarks: From Intrinsically Disordered Proteins to Alzheimer's Disease. *Adv. Exp. Med. Biol.* **2015**, *870*, 401–21.
(10) Darling, A. L.; Uversky, V. N. Intrinsic Disorder in Proteins with Pathogenic Repeat Expansions. *Molecules* **2017**, *22* (12), 2027.
(11) Iannuzzi, C.; Maritato, R.; Irace, G.; Sirangelo, I. Misfolding and amyloid aggregation of apomyoglobin. *Int. J. Mol. Sci.* **2013**, *14* (7), 14287–300.
(12) Chiti, F.; Dobson, C. M. Amyloid formation by globular proteins under native conditions. *Nat. Chem. Biol.* **2009**, *5* (1), 15–22.
(13) Iadanza, M. G.; Silvers, R.; Boardman, J.; Smith, H. I.; Karamanos, T. K.; Debelouchina, G. T.; Su, Y.; Griffin, R. G.; Ranson, N. A.; Radford, S. E. The structure of a beta2-microglobulin fibril suggests a molecular basis for its amyloid polymorphism. *Nat. Commun.* **2018**, *9* (1), 4517.
(14) Dember, L. M.; Jaber, B. L. Dialysis-related amyloidosis: late finding or hidden epidemic? *Semin Dial* **2006**, *19* (2), 105–9.
(15) Dzido, G.; Sprague, S. M. Dialysis-related amyloidosis. *Minerva Urol. Nefrol.* **2003**, *55* (2), 121–129.
(16) Gejyo, F.; Yamada, T.; Odani, S.; Nakagawa, Y.; Arakawa, M.; Kunitomo, T.; Kataoka, H.; Suzuki, M.; Hirasawa, Y.; Shirahama, T.; et al. A new form of amyloid protein associated with chronic hemodialysis was identified as beta 2-microglobulin. *Biochem. Biophys. Res. Commun.* **1985**, *129* (3), 701–6.
(17) Muñoz-Gómez, J.; Bergadá-Barado, E.; Gómez-Pérez, R.; Llopart-Buisán, E.; Subías-Sobrevía, E.; Rotés-Querol, J.; Solé-Arqués, M. Amyloid arthropathy in patients undergoing periodical haemo-

DOI: 10.1021/jacs.9b10421
J. Am. Chem. Soc. 2020, 142, 1321–1331

dialysis for chronic renal failure: a new complication. *Ann. Rheum. Dis.* **1985**, *44* (11), 729−733.
(18) Becker, J. W.; Reeke, G. N., Jr. Three-dimensional structure of beta 2-microglobulin. *Proc. Natl. Acad. Sci. U. S. A.* **1985**, *82* (12), 4225−9.
(19) Floege, J.; Bartsch, A.; Schulze, M.; Shaldon, S.; Koch, K. M.; Smeby, L. C. Clearance and synthesis rates of beta 2-microglobulin in patients undergoing hemodialysis and in normal subjects. *J. Lab Clin Med.* **1991**, *118* (2), 153−165.
(20) Homma, N.; Gejyo, F.; Isemura, M.; Arakawa, M. Collagen-binding affinity of beta-2-microglobulin, a preprotein of hemodialysis-associated amyloidosis. *Nephron* **2004**, *53* (1), 37−40.
(21) Relini, A.; Canale, C.; De Stefano, S.; Rolandi, R.; Giorgetti, S.; Stoppini, M.; Rossi, A.; Fogolari, F.; Corazza, A.; Esposito, G.; Gliozzi, A.; Bellotti, V. Collagen plays an active role in the aggregation of beta2-microglobulin under physiopathological conditions of dialysis-related amyloidosis. *J. Biol. Chem.* **2006**, *281* (24), 16521−9.
(22) Hadjipavlou, A.; Lander, P.; Begin, L.; Bercovitch, D.; Davidman, M.; Jakab, E. Skeletal amyloidosis due to beta microglobulinemia in a patient on hemodialysis. A case report. *J. Bone Joint Surg Am.* **1988**, *70* (1), 119−21.
(23) Bardin, T.; Kuntz, D.; Zingraff, J.; Voisin, M.-C.; Zelmar, A.; Lansaman, J. Synovial amyloidosis in patients undergoing long-term hemodialysis. *Arthritis Rheum.* **1985**, *28* (9), 1052−1058.
(24) Gejyo, F.; Odani, S.; Yamada, T.; Honma, N.; Saito, H.; Suzuki, Y.; Nakagawa, Y.; Kobayashi, H.; Maruyama, Y.; Hirasawa, Y.; et al. Beta 2-microglobulin: a new form of amyloid protein associated with chronic hemodialysis. *Kidney Int.* **1986**, *30* (3), 385−90.
(25) Eakin, C. M.; Miranker, A. D. From chance to frequent encounters: origins of beta2-microglobulin fibrillogenesis. *Biochim. Biophys. Acta, Proteins Proteomics* **2005**, *1753* (1), 92−9.
(26) Platt, G. W.; Radford, S. E. Glimpses of the molecular mechanisms of beta2-microglobulin fibril formation in vitro: aggregation on a complex energy landscape. *FEBS Lett.* **2009**, *583* (16), 2623−9.
(27) Moe, S. M.; Chen, N. X. The role of the synovium and cartilage in the pathogenesis of beta(2)-microglobulin amyloidosis. *Semin Dial* **2001**, *14* (2), 127−30.
(28) Relini, A.; De Stefano, S.; Torrassa, S.; Cavalleri, O.; Rolandi, R.; Gliozzi, A.; Giorgetti, S.; Raimondi, S.; Marchese, L.; Verga, L.; Rossi, A.; Stoppini, M.; Bellotti, V. Heparin strongly enhances the formation of beta2-microglobulin amyloid fibrils in the presence of type I collagen. *J. Biol. Chem.* **2008**, *283* (8), 4912−20.
(29) Benseny-Cases, N.; Karamanos, T. K.; Hoop, C. L.; Baum, J.; Radford, S. E. Extracellular matrix components modulate different stages in beta2-microglobulin amyloid formation. *J. Biol. Chem.* **2019**, *294* (24), 9392−9401.
(30) Giorgetti, S.; Rossi, A.; Mangione, P.; Raimondi, S.; Marini, S.; Stoppini, M.; Corazza, A.; Viglino, P.; Esposito, G.; Cetta, G.; Merlini, G.; Bellotti, V. Beta2-microglobulin isoforms display an heterogeneous affinity for type I collagen. *Protein Sci.* **2005**, *14* (3), 696−702.
(31) Myers, S. L.; Jones, S.; Jahn, T. R.; Morten, I. J.; Tennent, G. A.; Hewitt, E. W.; Radford, S. E. A systematic study of the effect of physiological factors on beta2-microglobulin amyloid formation at neutral pH. *Biochemistry* **2006**, *45* (7), 2311−21.
(32) Yamamoto, S.; Yamaguchi, I.; Hasegawa, K.; Tsutsumi, S.; Goto, Y.; Gejyo, F.; Naiki, H. Glycosaminoglycans enhance the trifluoroethanol-induced extension of beta 2-microglobulin-related amyloid fibrils at a neutral pH. *J. Am. Soc. Nephrol.* **2004**, *15* (1), 126−33.
(33) Srikanth, R.; Mendoza, V. L.; Bridgewater, J. D.; Zhang, G.; Vachet, R. W. Copper binding to beta-2-microglobulin and its pre-amyloid oligomers. *Biochemistry* **2009**, *48* (41), 9871−81.
(34) Antwi, K.; Mahar, M.; Srikanth, R.; Olbris, M. R.; Tyson, J. F.; Vachet, R. W. Cu(II) organizes beta-2-microglobulin oligomers but is released upon amyloid formation. *Protein Sci.* **2008**, *17* (4), 748−59.
(35) Calabrese, M. F.; Miranker, A. D. Metal binding sheds light on mechanisms of amyloid assembly. *Prion* **2009**, *3* (1), 1−4.
(36) Calabrese, M. F.; Eakin, C. M.; Wang, J. M.; Miranker, A. D. A regulatable switch mediates self-association in an immunoglobulin fold. *Nat. Struct. Mol. Biol.* **2008**, *15* (9), 965−71.
(37) Calabrese, M. F.; Miranker, A. D. Formation of a stable oligomer of beta-2 microglobulin requires only transient encounter with Cu(II). *J. Mol. Biol.* **2007**, *367* (1), 1−7.
(38) Jahn, T. R.; Parker, M. J.; Homans, S. W.; Radford, S. E. Amyloid formation under physiological conditions proceeds via a native-like folding intermediate. *Nat. Struct. Mol. Biol.* **2006**, *13* (3), 195−201.
(39) McParland, V. J.; Kad, N. M.; Kalverda, A. P.; Brown, A.; Kirwin-Jones, P.; Hunter, M. G.; Sunde, M.; Radford, S. E. Partially unfolded states of beta(2)-microglobulin and amyloid formation in vitro. *Biochemistry* **2000**, *39* (30), 8735−46.
(40) Morgan, C. J.; Gelfand, M.; Atreya, C.; Miranker, A. D. Kidney dialysis-associated amyloidosis: a molecular role for copper in fiber formation. *J. Mol. Biol.* **2001**, *309* (2), 339−45.
(41) Yamamoto, S.; Hasegawa, K.; Yamaguchi, I.; Tsutsumi, S.; Kardos, J.; Goto, Y.; Gejyo, F.; Naiki, H. Low concentrations of sodium dodecyl sulfate induce the extension of beta 2-microglobulin-related amyloid fibrils at a neutral pH. *Biochemistry* **2004**, *43* (34), 11075−82.
(42) Borysik, A. J.; Morten, I. J.; Radford, S. E.; Hewitt, E. W. Specific glycosaminoglycans promote unseeded amyloid formation from beta2-microglobulin under physiological conditions. *Kidney Int.* **2007**, *72* (2), 174−81.
(43) Gosal, W. S.; Morten, I. J.; Hewitt, E. W.; Smith, D. A.; Thomson, N. H.; Radford, S. E. Competing pathways determine fibril morphology in the self-assembly of beta2-microglobulin into amyloid. *J. Mol. Biol.* **2005**, *351* (4), 850−64.
(44) Ricagno, S.; Colombo, M.; de Rosa, M.; Sangiovanni, E.; Giorgetti, S.; Raimondi, S.; Bellotti, V.; Bolognesi, M. DE loop mutations affect beta2-microglobulin stability and amyloid aggregation. *Biochem. Biophys. Res. Commun.* **2008**, *377* (1), 146−150.
(45) Santambrogio, C.; Ricagno, S.; Colombo, M.; Barbiroli, A.; Bonomi, F.; Bellotti, V.; Bolognesi, M.; Grandori, R. DE-loop mutations affect beta2 microglobulin stability, oligomerization, and the low-pH unfolded form. *Protein Sci.* **2010**, *19* (7), 1386−94.
(46) Halabelian, L.; Relini, A.; Barbiroli, A.; Penco, A.; Bolognesi, M.; Ricagno, S. A covalent homodimer probing early oligomers along amyloid aggregation. *Sci. Rep.* **2015**, *5*, 14651.
(47) Leney, A. C.; Pashley, C. L.; Scarff, C. A.; Radford, S. E.; Ashcroft, A. E. Insights into the role of the beta-2 microglobulin D-strand in amyloid propensity revealed by mass spectrometry. *Mol. BioSyst.* **2014**, *10* (3), 412−20.
(48) Narang, D.; Singh, A.; Swasthi, H. M.; Mukhopadhyay, S. Characterization of Salt-Induced Oligomerization of Human beta2-Microglobulin at Low pH. *J. Phys. Chem. B* **2016**, *120* (32), 7815−23.
(49) Eichner, T.; Kalverda, A. P.; Thompson, G. S.; Homans, S. W.; Radford, S. E. Conformational conversion during amyloid formation at atomic resolution. *Mol. Cell* **2011**, *41* (2), 161−72.
(50) Kameda, A.; Hoshino, M.; Higurashi, T.; Takahashi, S.; Naiki, H.; Goto, Y. Nuclear magnetic resonance characterization of the refolding intermediate of beta2-microglobulin trapped by non-native prolyl peptide bond. *J. Mol. Biol.* **2005**, *348* (2), 383−97.
(51) Sakata, M.; Chatani, E.; Kameda, A.; Sakurai, K.; Naiki, H.; Goto, Y. Kinetic coupling of folding and prolyl isomerization of beta2-microglobulin studied by mutational analysis. *J. Mol. Biol.* **2008**, *382* (5), 1242−55.
(52) Janowska, M. K.; Wu, K. P.; Baum, J. Unveiling transient protein-protein interactions that modulate inhibition of alpha-synuclein aggregation by beta-synuclein, a pre-synaptic protein that co-localizes with alpha-synuclein. *Sci. Rep.* **2015**, *5*, 15164.
(53) Wu, K. P.; Baum, J. Detection of transient interchain interactions in the intrinsically disordered protein alpha-synuclein by NMR paramagnetic relaxation enhancement. *J. Am. Chem. Soc.* **2010**, *132* (16), 5546−7.
(54) Lian, L. Y. NMR studies of weak protein-protein interactions. *Prog. Nucl. Magn. Reson. Spectrosc.* **2013**, *71*, 59−72.

DOI: 10.1021/jacs.9b10421
J. Am. Chem. Soc. 2020, 142, 1321−1331

(55) Vinogradova, O.; Qin, J. NMR as a unique tool in assessment and complex determination of weak protein-protein interactions. *Top. Curr. Chem.* **2011**, *326*, 35−45.
(56) Fawzi, N. L.; Ying, J.; Ghirlando, R.; Torchia, D. A.; Clore, G. M. Atomic-resolution dynamics on the surface of amyloid-beta protofibrils probed by solution NMR. *Nature* **2011**, *480* (7376), 268−72.
(57) Fawzi, N. L.; Ying, J.; Torchia, D. A.; Clore, G. M. Probing exchange kinetics and atomic resolution dynamics in high-molecular-weight complexes using dark-state exchange saturation transfer NMR spectroscopy. *Nat. Protoc.* **2012**, *7* (8), 1523−33.
(58) Karamanos, T. K.; Kalverda, A. P.; Thompson, G. S.; Radford, S. E. Visualization of transient protein-protein interactions that promote or inhibit amyloid assembly. *Mol. Cell* **2014**, *55* (2), 214−26.
(59) Le Marchand, T.; de Rosa, M.; Salvi, N.; Sala, B. M.; Andreas, L. B.; Barbet-Massin, E.; Sormanni, P.; Barbiroli, A.; Porcari, R.; Sousa Mota, C.; de Sanctis, D.; Bolognesi, M.; Emsley, L.; Bellotti, V.; Blackledge, M.; Camilloni, C.; Pintacuda, G.; Ricagno, S. Conformational dynamics in crystals reveal the molecular bases for D76N beta-2 microglobulin aggregation propensity. *Nat. Commun.* **2018**, *9* (1), 1658.
(60) Camilloni, C.; Sala, B. M.; Sormanni, P.; Porcari, R.; Corazza, A.; De Rosa, M.; Zanini, S.; Barbiroli, A.; Esposito, G.; Bolognesi, M.; Bellotti, V.; Vendruscolo, M.; Ricagno, S. Rational design of mutations that change the aggregation rate of a protein while maintaining its native structure and stability. *Sci. Rep.* **2016**, *6*, 25559.
(61) Jahn, T. R.; Tennent, G. A.; Radford, S. E. A common beta-sheet architecture underlies in vitro and in vivo beta2-microglobulin amyloid fibrils. *J. Biol. Chem.* **2008**, *283* (25), 17279−86.
(62) Orgel, J. P.; Irving, T. C.; Miller, A.; Wess, T. J. Microfibrillar structure of type I collagen in situ. *Proc. Natl. Acad. Sci. U. S. A.* **2006**, *103* (24), 9001−5.
(63) Merck, E.; Gaillard, C.; Gorman, D. M.; Montero-Julian, F.; Durand, I.; Zurawski, S. M.; Menetrier-Caux, C.; Carra, G.; Lebecque, S.; Trinchieri, G.; Bates, E. E. OSCAR is an FcRgamma-associated receptor that is expressed by myeloid cells and is involved in antigen presentation and activation of human dendritic cells. *Blood* **2004**, *104* (5), 1386−95.
(64) Kim, N.; Takami, M.; Rho, J.; Josien, R.; Choi, Y. A novel member of the leukocyte receptor complex regulates osteoclast differentiation. *J. Exp. Med.* **2002**, *195* (2), 201−9.
(65) Meyaard, L.; Hurenkamp, J.; Clevers, H.; Lanier, L. L.; Phillips, J. H. Leukocyte-associated Ig-like receptor-1 functions as an inhibitory receptor on cytotoxic T cells. *J. Immunol* **1999**, *162* (10), 5800−5804.
(66) Poggi, A.; Tomasello, E.; Ferrero, E.; Zocchi, M. R.; Moretta, L. p40/LAIR-1 regulates the differentiation of peripheral blood precursors to dendritic cells induced by granulocyte-monocyte colony-stimulating factor. *Eur. J. Immunol.* **1998**, *28* (7), 2086−91.
(67) Ruggeri, Z. M. Platelets in atherothrombosis. *Nat. Med.* **2002**, *8* (11), 1227−34.
(68) Moroi, M.; Jung, S. M. Platelet glycoprotein VI: its structure and function. *Thromb. Res.* **2004**, *114* (4), 221−33.
(69) Kahn, M. L. Platelet-collagen responses: molecular basis and therapeutic promise. *Semin. Thromb. Hemostasis* **2004**, *30* (4), 419−25.
(70) Zhou, L.; Hinerman, J. M.; Blaszczyk, M.; Miller, J. L.; Conrady, D. G.; Barrow, A. D.; Chirgadze, D. Y.; Bihan, D.; Farndale, R. W.; Herr, A. B. Structural basis for collagen recognition by the immune receptor OSCAR. *Blood* **2016**, *127* (5), 529−37.
(71) Lebbink, R. J.; Raynal, N.; de Ruiter, T.; Bihan, D. G.; Farndale, R. W.; Meyaard, L. Identification of multiple potent binding sites for human leukocyte associated Ig-like receptor LAIR on collagens II and III. *Matrix Biol.* **2009**, *28* (4), 202−10.
(72) Brondijk, T. H.; de Ruiter, T.; Ballering, J.; Wienk, H.; Lebbink, R. J.; van Ingen, H.; Boelens, R.; Farndale, R. W.; Meyaard, L.; Huizinga, E. G. Crystal structure and collagen-binding site of immune inhibitory receptor LAIR-1: unexpected implications for collagen binding by platelet receptor GPVI. *Blood* **2010**, *115* (7), 1364−73.
(73) Smethurst, P. A.; Joutsi-Korhonen, L.; O'Connor, M. N.; Wilson, E.; Jennings, N. S.; Garner, S. F.; Zhang, Y.; Knight, C. G.; Dafforn, T. R.; Buckle, A.; MJ, I. J.; De Groot, P. G.; Watkins, N. A.; Farndale, R. W.; Ouwehand, W. H. Identification of the primary collagen-binding surface on human glycoprotein VI by site-directed mutagenesis and by a blocking phage antibody. *Blood* **2004**, *103* (3), 903−911.
(74) Horii, K.; Kahn, M. L.; Herr, A. B. Structural basis for platelet collagen responses by the immune-type receptor glycoprotein VI. *Blood* **2006**, *108* (3), 936−42.
(75) O'Connor, M. N.; Smethurst, P. A.; Farndale, R. W.; Ouwehand, W. H. Gain- and loss-of-function mutants confirm the importance of apical residues to the primary interaction of human glycoprotein VI with collagen. *J. Thromb. Haemostasis* **2006**, *4* (4), 869−73.
(76) Eichner, T.; Radford, S. E. Understanding the complex mechanisms of beta2-microglobulin amyloid assembly. *FEBS J.* **2011**, *278* (20), 3868−83.
(77) Verdone, G.; Corazza, A.; Viglino, P.; Pettirossi, F.; Giorgetti, S.; Mangione, P.; Andreola, A.; Stoppini, M.; Bellotti, V.; Esposito, G. The solution structure of human beta2-microglobulin reveals the prodromes of its amyloid transition. *Protein Sci.* **2002**, *11* (3), 487−99.
(78) Ricagno, S.; Raimondi, S.; Giorgetti, S.; Bellotti, V.; Bolognesi, M. Human beta-2 microglobulin W60V mutant structure: Implications for stability and amyloid aggregation. *Biochem. Biophys. Res. Commun.* **2009**, *380* (3), 543−7.
(79) Esposito, G.; Corazza, A.; Viglino, P.; Verdone, G.; Pettirossi, F.; Fogolari, F.; Makek, A.; Giorgetti, S.; Mangione, P.; Stoppini, M.; Bellotti, V. Solution structure of beta(2)-microglobulin and insights into fibrillogenesis. *Biochim. Biophys. Acta, Proteins Proteomics* **2005**, *1753* (1), 76−84.
(80) Trinh, C. H.; Smith, D. P.; Kalverda, A. P.; Phillips, S. E.; Radford, S. E. Crystal structure of monomeric human beta-2-microglobulin reveals clues to its amyloidogenic properties. *Proc. Natl. Acad. Sci. U. S. A.* **2002**, *99* (15), 9771−6.
(81) Hodkinson, J. P.; Jahn, T. R.; Radford, S. E.; Ashcroft, A. E. HDX-ESI-MS reveals enhanced conformational dynamics of the amyloidogenic protein beta(2)-microglobulin upon release from the MHC-1. *J. Am. Soc. Mass Spectrom.* **2009**, *20* (2), 278−86.
(82) Rennella, E.; Corazza, A.; Fogolari, F.; Viglino, P.; Giorgetti, S.; Stoppini, M.; Bellotti, V.; Esposito, G. Equilibrium unfolding thermodynamics of beta2-microglobulin analyzed through native-state H/D exchange. *Biophys. J.* **2009**, *96* (1), 169−79.
(83) Rennella, E.; Corazza, A.; Giorgetti, S.; Fogolari, F.; Viglino, P.; Porcari, R.; Verga, L.; Stoppini, M.; Bellotti, V.; Esposito, G. Folding and fibrillogenesis: clues from beta2-microglobulin. *J. Mol. Biol.* **2010**, *401* (2), 286−97.
(84) Armen, R. S.; Daggett, V. Characterization of two distinct beta2-microglobulin unfolding intermediates that may lead to amyloid fibrils of different morphology. *Biochemistry* **2005**, *44* (49), 16098−107.
(85) Fogolari, F.; Corazza, A.; Viglino, P.; Zuccato, P.; Pieri, L.; Faccioli, P.; Bellotti, V.; Esposito, G. Molecular dynamics simulation suggests possible interaction patterns at early steps of beta2-microglobulin aggregation. *Biophys. J.* **2007**, *92* (5), 1673−81.
(86) Corazza, A.; Rennella, E.; Schanda, P.; Mimmi, M. C.; Cutuil, T.; Raimondi, S.; Giorgetti, S.; Fogolari, F.; Viglino, P.; Frydman, L.; Gal, M.; Bellotti, V.; Brutscher, B.; Esposito, G. Native-unlike long-lived intermediates along the folding pathway of the amyloidogenic protein beta2-microglobulin revealed by real-time two-dimensional NMR. *J. Biol. Chem.* **2010**, *285* (8), 5827−35.
(87) Chiti, F.; De Lorenzi, E.; Grossi, S.; Mangione, P.; Giorgetti, S.; Caccialanza, G.; Dobson, C. M.; Merlini, G.; Ramponi, G.; Bellotti, V. A partially structured species of beta 2-microglobulin is significantly populated under physiological conditions and involved in fibrillogenesis. *J. Biol. Chem.* **2001**, *276* (50), 46714−21.
(88) Chiti, F.; Mangione, P.; Andreola, A.; Giorgetti, S.; Stefani, M.; Dobson, C. M.; Bellotti, V.; Taddei, N. Detection of two partially

DOI: 10.1021/jacs.9b10421
J. Am. Chem. Soc. 2020, 142, 1321−1331

structured species in the folding process of the amyloidogenic protein beta 2-microglobulin. *J. Mol. Biol.* **2001**, *307* (1), 379−91.
(89) Esposito, G.; Michelutti, R.; Verdone, G.; Viglino, P.; Hernandez, H.; Robinson, C. V.; Amoresano, A.; Dal Piaz, F.; Monti, M.; Pucci, P.; Mangione, P.; Stoppini, M.; Merlini, G.; Ferri, G.; Bellotti, V. Removal of the N-terminal hexapeptide from human beta2-microglobulin facilitates protein aggregation and fibril formation. *Protein Sci.* **2000**, *9* (5), 831−845.
(90) Monti, M.; Amoresano, A.; Giorgetti, S.; Bellotti, V.; Pucci, P. Limited proteolysis in the investigation of beta2-microglobulin amyloidogenic and fibrillar states. *Biochim. Biophys. Acta, Proteins Proteomics* **2005**, *1753* (1), 44−50.
(91) Mangione, P. P.; Esposito, G.; Relini, A.; Raimondi, S.; Porcari, R.; Giorgetti, S.; Corazza, A.; Fogolari, F.; Penco, A.; Goto, Y.; Lee, Y. H.; Yagi, H.; Cecconi, C.; Naqvi, M. M.; Gillmore, J. D.; Hawkins, P. N.; Chiti, F.; Rolandi, R.; Taylor, G. W.; Pepys, M. B.; Stoppini, M.; Bellotti, V. Structure, folding dynamics, and amyloidogenesis of D76N beta2-microglobulin: roles of shear flow, hydrophobic surfaces, and alpha-Crystallin. *J. Biol. Chem.* **2013**, *288* (43), 30917−30.
(92) Johnson, S. M.; Connelly, S.; Fearns, C.; Powers, E. T.; Kelly, J. W. The transthyretin amyloidoses: from delineating the molecular mechanism of aggregation linked to pathology to a regulatory-agency-approved drug. *J. Mol. Biol.* **2012**, *421* (2−3), 185−203.
(93) Delaglio, F.; Grzesiek, S.; Vuister, G. W.; Zhu, G.; Pfeifer, J.; Bax, A. NMRPipe: a multidimensional spectral processing system based on UNIX pipes. *J. Biomol. NMR* **1995**, *6* (3), 277−293.
(94) Goddard, T. D.; Kneller, D. G. *SPARKY* 3; University of California: San Fransisco, CA, 2008.
(95) Palmer, A. G.; Cavanagh, J.; Wright, P. E.; Rance, M. Sensitivity improvement in proton-detected two-dimensional heteronuclear correlation NMR spectroscopy. *J. Magn. Reson. (1969-1992)* **1991**, *93* (1), 151−170.
(96) Kay, L.; Keifer, P.; Saarinen, T. Pure absorption gradient enhanced heteronuclear single quantum correlation spectroscopy with improved sensitivity. *J. Am. Chem. Soc.* **1992**, *114* (26), 10663−10665.
(97) Hansen, D. F.; Vallurupalli, P.; Kay, L. E. An improved 15N relaxation dispersion experiment for the measurement of millisecond time-scale dynamics in proteins. *J. Phys. Chem. B* **2008**, *112* (19), 5898−904.
(98) Millet, O.; Loria, J. P.; Kroenke, C. D.; Pons, M.; Palmer, A. G. The static magnetic field dependence of chemical exchange linebroadening defines the NMR chemical shift time scale. *J. Am. Chem. Soc.* **2000**, *122* (12), 2867−2877.

DOI: 10.1021/jacs.9b10421
J. Am. Chem. Soc. 2020, 142, 1321−1331